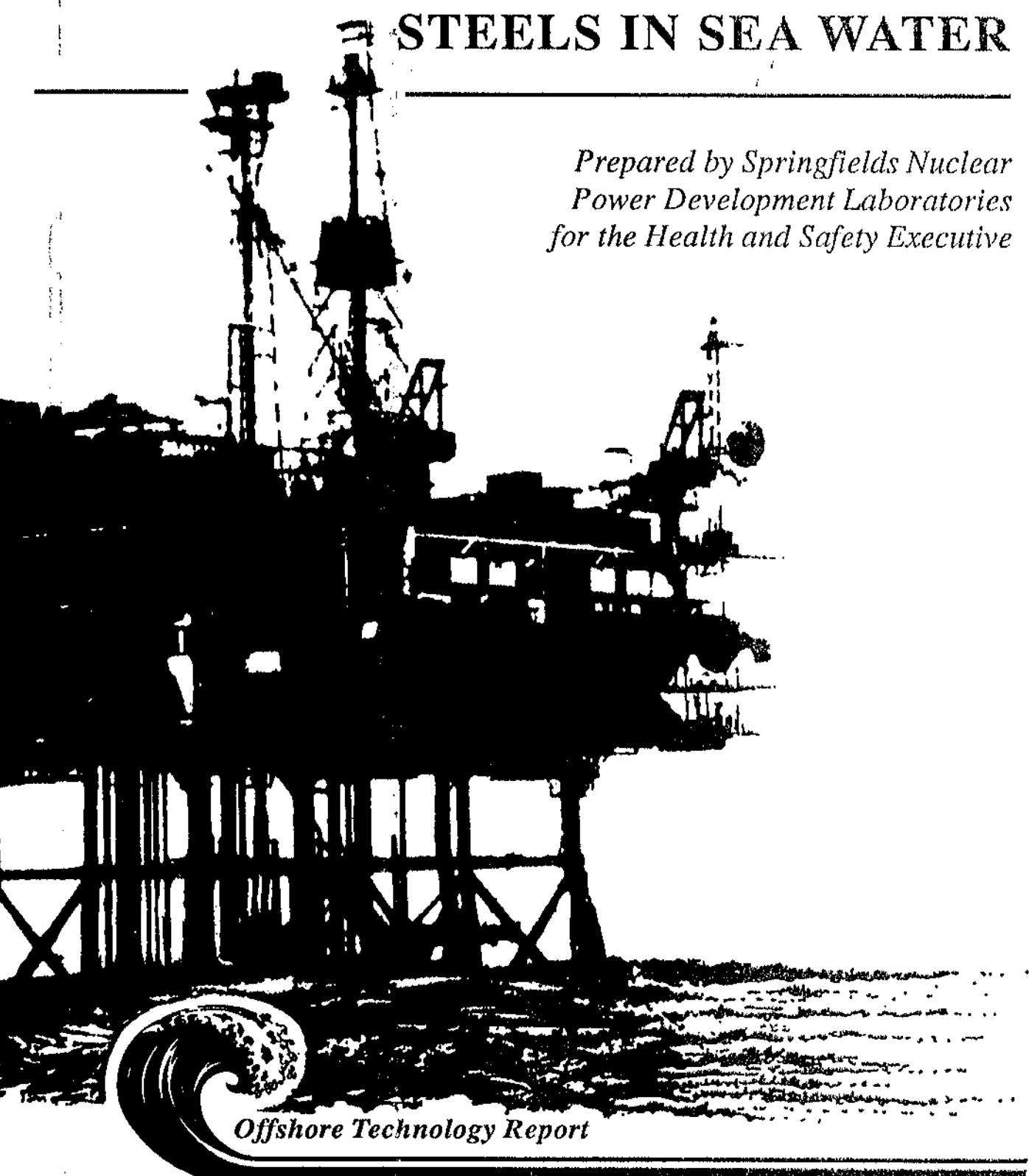




EFFECTS OF CATHODIC PROTECTION POTENTIAL AND STRESS RATIO ON FATIGUE THRESHOLDS OF STRUCTURED STEELS IN SEA WATER

Prepared by Springfields Nuclear Power Development Laboratories for the Health and Safety Executive



Offshore Technology Report

Health and Safety Executive

**EFFECTS OF CATHODIC
PROTECTION POTENTIAL AND
STRESS RATIO ON FATIGUE
THRESHOLDS OF STRUCTURED
STEELS IN SEA WATER**

Authors

A S Dolphin and D R Tice

*Springfields Nuclear Power Development Laboratories
Salwick, Preston PR4 0RR*

This report is published by the Health and Safety Executive as part of a series of reports of work which has been supported by funds formerly provided by the Department of Energy and lately by the Executive. Neither the Executive, the Department nor the contractors concerned assume any liability for the reports nor do they necessarily reflect the views or policy of the Executive or the Department.

Results, including detailed evaluation and, where relevant, recommendations stemming from their research projects are published in the OTH series of reports.

Background information and data arising from these research projects are published in the OTI series of reports.

HMSO

Standing order service

Placing a standing order with HMSO BOOKS enables a customer to receive other titles in this series automatically as published. This saves time, trouble and expense of placing individual orders and avoids the problem of knowing when to do so.

For details please write to HMSO BOOKS (PC 13A/1),
Publications Centre, PO Box 276, London SW8 5DT quoting
reference 12.01.025

The standing order service also enables customers to receive automatically as published all material of their choice which additionally saves extensive catalogue research. The scope and selectivity of the service has been extended by new techniques, and there are more than 3,500 classifications to choose from. A special leaflet describing the service in detail may be obtained on request.

CONTENTS

SUMMARY	5
1. INTRODUCTION	7
2. EXPERIMENTAL DETAILS	9
2.1 MATERIAL, SPECIMENS AND TEST MACHINES	9
2.2 TEST ENVIRONMENT	10
2.3 TESTING PROCEDURE	11
2.4 DATA ANALYSIS	11
3. RESULTS	13
3.1 THROUGH THICKNESS CRACKED SPECIMEN TESTS	13
3.2 SEMI-ELLIPTICAL CRACKED SPECIMENS	14
3.3 ANALYSIS OF THE SURFACE DEPOSITS IN CTS TESTS USING EMPA	14
4. DISCUSSION	17
4.1 EFFECT OF TEST PROCEDURE	17
4.2 EFFECT OF R-RATIO	17
4.3 EFFECT OF CATHODIC PROTECTION POTENTIAL	18
4.4 EFFECT OF SPECIMEN GEOMETRY	18
5. CONCLUSIONS	21
6. RECOMMENDATIONS	23
7. REFERENCES	25
TABLES 1-3	26
FIGURES 1-8	29

SUMMARY

The threshold stress intensity range for corrosion fatigue crack growth is an important parameter for the prediction of in service crack propagation in offshore structures in the North Sea by fracture mechanics techniques. This memorandum describes the results of an investigation into the influence of test technique, stress ratio, cathodic protection potential and specimen geometry on corrosion fatigue crack growth thresholds of BS 4360: 50D steel in natural seawater.

The results indicate a large effect of the method of testing (i.e. increasing vs decreasing stress intensity range) at cathodic protection potentials which result in only mild calcareous scale formation (-0.85 V (SCE)). At more negative potentials, (-1.05 V (SCE)), scaling has a major effect on crack growth. Preliminary results on specimens with semi-elliptical cracks indicate broadly similar near-threshold crack growth rates to those of through thickness cracks in the compact tension specimens used for the remainder of the programme.

1
2
3
4
5
6
7
8
9
10
11
12
13
14
15
16
17
18
19
20
21
22
23
24
25
26
27
28
29
30
31
32
33
34
35
36
37
38
39
40
41
42
43
44
45
46
47
48
49
50
51
52
53
54
55
56
57
58
59
60
61
62
63
64
65
66
67
68
69
70
71
72
73
74
75
76
77
78
79
80
81
82
83
84
85
86
87
88
89
90
91
92
93
94
95
96
97
98
99
100

1. INTRODUCTION

Since the late nineteen sixties and early seventies when the North Sea oil reserves were first being explored and exploited, avoidance of failure due to fatigue has always been a major element in providing safe designs. This constraint, added to the poor applicability of experience gained from less extreme environments has given a large impetus to fatigue and corrosion fatigue testing and research. One area of particular importance has been the application of fracture mechanics and crack growth concepts which are valuable for damage tolerant design and also for inspection engineering. Considerable progress has been achieved in providing relevant and reliable fatigue information under North sea conditions but, despite this work, important gaps in understanding remain.

One subject of importance is the knowledge of the threshold stress intensity range for fatigue crack growth. The existence of such a threshold can have very important implications in the early and middle life of offshore structures. Whilst a substantial proportion of the life of a small specimen used for conventional fatigue testing is spent in crack initiation, in practice it is not possible to guarantee that real structures will not contain crack like defects, especially in the regions of welds, and it is usually assumed that a crack of the limiting size for detection by nondestructive examination (NDE) techniques is present. However, the crack size and load regime may be such that any defects would experience stress intensities at or near the threshold of crack growth for a large proportion of the service life of the structure. Therefore a knowledge of the rate at which pre-existing cracks will grow enables a more accurate assessment of the lifetime of a defected component. Such an assessment becomes increasingly important for safety assurance with the advancing age of existing structures, particularly when consideration of alternative uses of a platform are made once oil production stops.

This appreciation of the importance of crack growth thresholds has led to a great deal of work being concentrated on this topic; witnessed by the increased number of publications on threshold measurement during the early nineteen eighties¹. Threshold testing of BS 4360 - 50D steel was an important part of the UK's Department of Energy funded work. In this work, fatigue thresholds and crack growth rates were measured in realistic marine conditions². Fatigue thresholds were measured using a reducing stress intensity technique, over a range of stress ratios ($R = -1$ to 0.5) in bulk freely corroding and cathodically protected conditions. However, there were some remaining gaps in the database, viz the effects of high stress ratio ($R > 0.5$) and fully reversed load ($R = -1$) data under cathodic protection conditions. Additionally, no data were obtained under cathodic overprotection conditions.

Another series of tests was undertaken, which form the basis of the work reported here. However, during the period immediately preceding the start of testing, an important change was made in the test technique. As stated above, measurements of thresholds in the original project were made by reducing the stress intensity until crack growth became essentially undetectable i.e. a crack growth rate below 10^{-11} m/cycle. Subsequently this method has been criticised for not being representative of the practical situation where stress intensity would be expected to increase during the life of a structure. Hence a modified test technique was adopted for the current work in an attempt to more closely simulate the rising stress intensity expected for components in service. However, it should be noted that this procedure does not truly simulate service conditions of variable amplitude loading.

When a component is subjected to fatigue in sea water there are two competitive influences of the environment, in addition to the mechanical contribution to crack growth. One of the factors which will govern the rate of crack propagation is the formation of deposits on the fracture surface, notably calcareous scale, particularly under cathodic protection. Formation of deposits on the fracture surface is likely to have a beneficial effect in reducing the effective loads at the crack tip and hence reduce crack growth rates. However, such deposits can form and behave in an unpredictable manner, resulting in an inconsistent response, particularly at low stress intensities where scale may be more effective in causing crack closure effects. Contrasting with this effect is the aggressive nature of the sea water which can increase crack growth rates over those in air. Recent work investigating the electrochemical conditions within corrosion fatigue cracks in sea water indicates that hydrogen has an important effect in enhancing crack growth. Additionally, because hydrogen concentration within a specimen is governed by diffusion rates which are difficult to measure, it is possible that an equilibrium concentration is not reached during relatively short term corrosion fatigue tests. Therefore in such tests the full effects of enhanced crack growth rate due to hydrogen might not be measured.

This memorandum describes fully the work carried out and compares the results with those obtained not only in the previous programme², but also by other workers on BS4360:50D structural steel in marine environments.

2. EXPERIMENTAL DETAILS

2.1 MATERIAL, SPECIMENS AND TEST MACHINES

To maintain consistency with previous work, the same steel was used. This material was manufactured by the British Steel Corporation to BS4360:50D³ in the form of 38 mm thick plate whose pedigree was determined by the Welding Institute, composition shown in Table 1. Because the steel was produced in the early 1970's it has higher sulphur and phosphorous content than modern steels and this is likely to degrade mechanical properties particularly in the through-thickness direction, but it was considered that the results obtained would be representative of many offshore structures which were fabricated from steel of the same vintage. Specimens manufactured from the plate were oriented so that crack growth was perpendicular to the rolling direction. Both compact tension and four point bend specimens were tested in the L-S orientation.

Two types of specimen were used; a compact tension specimen (CTS) and a four point bend specimen with a semi-elliptical crack. Specimen dimensions are given in Figs 1 and 2. The cyclic stress intensity factor, ΔK , for the CTS was calculated using the compliance calibration:

$$\Delta K = \frac{\Delta P Y}{B\sqrt{W}} \quad (\text{MPa } \sqrt{\text{m}})$$

Where:

ΔP = Applied load range (N)

W = Specimen width (from the load line to the back of the specimen)

B = Specimen thickness (m)

Y = The compliance function, which is given by:

$$Y = 29.6 \left(\frac{a}{W}\right)^{1/2} - 185.5 \left(\frac{a}{W}\right)^{3/2} + 655.7 \left(\frac{a}{W}\right)^{5/2} - 1017 \left(\frac{a}{W}\right)^{7/2} + 638.9 \left(\frac{a}{W}\right)^{9/2}$$

The stress intensity ranges were calculated for the bend specimen both at the surface and depth using equations based on the work of Scott & Thorpe⁴.

For the depth stress intensity range

$$\Delta K_{(\Theta=90^\circ)} = \frac{M}{E(k)} \left\{ 1 - 1.36 \left(\frac{a}{t}\right), \left(\frac{a}{c}\right)^{0.1} \right\} \frac{2t \Delta P \sqrt{\pi a}}{Wt^2}$$

Where:

$$M = 1.13 - 0.07 \left(\frac{a}{c}\right)^{1/2}$$

$$E(k) = 1 + 1.47 \left(\frac{a}{c}\right)^{1.64}$$

a = Crack depth

c = Half the total surface crack length

For the surface stress intensity range

$$\Delta K_{(\Theta=0)} = \left\{ M_1 \left(1 - 0.3 \left(\frac{a}{r} \right) \left(1 - \left(\frac{a}{t} \right)^2 \right) + \left[0.394 \times E(k) \left(\frac{a}{r} \right)^2 \cdot \left(\frac{c}{a} \right)^{1/2} \right] \right\} \times \left\{ \frac{2L \Delta P \sqrt{\pi a}}{E(k) W t^2} \right\}$$

Where:

$$M_1 = \left[1.21 - 0.1 \left(\frac{a}{c} \right) + 0.1 \left(\frac{a}{c} \right)^4 \right] \left(\frac{a}{c} \right)^{1/2}$$

$$E(k) = 1 + 1.47 \left(\frac{a}{c} \right)^{1.64}$$

Crack length measurements for the CTS were made by optical inspection using a microscope which contained a calibrated graticule in combination with reference lines scribed on the specimen surface. This technique gave a resolution in crack length of 0.04 mm when used by an experienced operator. These crack length measurements were taken on both surfaces and were corrected after the test by use of the beach marks on the fracture surfaces as calibration points, to provide a value for mean crack length across the crack front. However, it was not possible to use this optical technique for measuring crack growth in the bend specimens, hence the alternating current potential drop (A.C.P.D) technique was adopted. The relatively small size of this test piece prevented large numbers of potential measurement probes being attached which precluded measurement of the surface crack length. The length of the crack on the specimen surface was calculated after the test assuming a relationship between the length and depth of the crack as reported by Scott and Thorpe⁴. The applicability of this assumption was checked using beach marks made on the specimen surface after pre-cracking and at the end of the test.

All the tests were performed on servo hydraulic testing machines; the CTS tests were done on two machines with a maximum capacity of 50 kN while the tests using bend specimens employed a machine with 100 kN capacity.

2.2 TEST ENVIRONMENT

All the tests were performed in natural sea water with impressed current cathodic protection. The water used was obtained from the English Channel and circulated through an aeration system and chiller which maintained the temperature in each test cell at $7 \pm 0.5^\circ\text{C}$. The seawater was recirculated through each perspex test cell at about 2 litres per minute from a tank containing about 1500 litres, with the total volume of this tank being replaced at quarterly intervals. Cathodic protection was applied using potentiostatic control with two platinum foil counter electrodes placed parallel to the specimen sides, one either side. Potential was set using a saturated calomel electrode (SCE) located close to the notch mouth. A second SCE was used to sample the potential within the notch area at intervals during the test. Two protection potentials were used with the CTS, -0.85 V and -1.05 V (SCE), while the semi-elliptically cracked specimens were only tested at -0.85 V (SCE). The compact tension specimens were insulated from the grip assembly by Tufnol bushes. Leather strips insulated the bend specimens, although only the central portions of these specimens away from the loading points were in contact with the seawater.

2.3 TESTING PROCEDURE

The original aim of the work described in this report was to provide additional data to supplement the results from the earlier work². In the earlier work, crack growth thresholds were measured by reducing the stress intensity range either manually, or using a constant backface strain technique. While the measurement of thresholds under reducing stress intensity may be quite satisfactory in inert environments, the technique becomes more questionable where the test is done in an environment where deposits can form on the fracture surface. Secondly, the reducing load regime less accurately models behaviour in real components where cracks would experience increasing average stress intensities. For these reasons it was decided to change the test procedure of this work to model more closely the practical situation. The stages in the test method used in the current project are outlined below.

- (a) The specimen was pre-cracked in the test environment using a cyclic frequency of 5 Hz.
- (b) The crack growth rate was reduced using step reductions of load until a threshold ΔK was reached at 5 Hz, again in the test environment.
- (c) When the threshold had been reached, the cyclic frequency was reduced to 0.167 Hz. After more than 120,000 fatigue cycles had been achieved the stress intensity was increased in 10% steps until measurable growth of about 0.1 mm occurred.

The modified test procedure was designed to achieve threshold under reducing load conditions with little enhancement of the crack growth rate from the environment, hence the use of a relatively high loading frequency of 5 Hz.

Conducting the precracking stage in sea water provided time for the environmental conditions to achieve steady state, except within the crack. Once threshold had been achieved, the cyclic frequency was reduced to a value more representative of service conditions, where the environment was expected to enhance crack propagation rates.

This revised procedure was expected to produce near threshold crack growth rates which more accurately reflected those experienced in service. However, substantial differences between the results using the two test procedures were not expected, so the matrix of tests planned in this project did not duplicate any done previously, as shown in Table 2.

2.4 DATA ANALYSIS

The operation of crack growth threshold testing and measurement of near threshold growth rates necessarily means that very small amounts of growth occur. Small amounts of crack growth ensure that errors associated with the resolution and repeatability of the crack length measuring system become a significant factor in the results obtained. Therefore careful interpretation of the measured data is essential prior to calculating growth rate values. This was achieved by manual fitting of tangents to crack length vs fatigue cycles ($a-N$) data.

Consideration of the errors associated with crack length measurement using the optical technique suggest a resolution of 0.04 mm is possible, under ideal conditions. To obtain this resolution requires a well polished specimen surface at the start of the test, which must be kept free of corrosion deposits etc. by use of a nylon bristle bush. It is also necessary for

there to be a close correspondence between the surface crack growth and the growth through the thickness, i.e. no significant crack front tunnelling. Corrections can be applied after testing to account for any increase or decrease in crack curvature during growth along the specimen, by reference to beach marks on the surface, but this technique could only be applied to CT specimens where the crack sides were exposed and access to view them possible. Measurement of the crack depth on the semi-elliptical crack bend specimens had to rely upon A.C.P.D methods. The resolution of this technique using the available hardware was found to be of the order of ± 0.2 mm, which is large relative to the crack growth rate that can be achieved in threshold test work. Testing times at 0.167 Hz would be very extended at near threshold crack growth rates before crack advance could be assured. Data obtained from these specimens, therefore, can be regarded only as an indication of trends rather than quantitative data to be used for assessment purposes.

3. RESULTS

3.1 THROUGH THICKNESS CRACKED SPECIMEN TESTS

Five tests have been performed using 25 mm thick compact tension specimens at two protection potentials, -0.85 V (SCE) and -1.05 V (SCE).

(a) - 0.85 V, R = 0.7

Crack growth data at 0.0167 Hz under increasing ΔK conditions are shown in Fig. 3. These data indicate a threshold stress intensity range of around 4.8 MPa \sqrt{m} . For this test only, cathodic protection was not applied during the pre-cracking stage in seawater but was established during the load reduction stages at 5 Hz. For all other tests cathodic protection was maintained from the start. During the month while the specimen was brought to threshold conditions, about 7 mm of crack growth was measured. Therefore the initial period of pre-cracking without cathodic protection is not believed to have had a significant influence on the measured threshold.

(b) - 0.85 V, R = 0

Operation of $R = 0$ tests using CTS geometry is not practical hence the actual R was maintained within a range between 0.05 and 0.1 . These values are sufficiently close to zero to allow the data to be representative of data at $R = 0$. The crack growth data for this test under increasing ΔK are also shown in Fig. 3. While there are no data at very low growth rates, a stress intensity value of 10 to 11 MPa \sqrt{m} appears to be an upper bound to the threshold value. During the load reduction stage of this test, one side of the crack reached an apparent threshold well before the opposite side, which continued to grow at lower loads. The fracture surface, revealed after testing, indicated that crack arrest had only occurred over about one third to one quarter of the specimen thickness. The results quoted in Figure 3 are based on growth rates calculated from the crack side which continued to grow.

(c) - 1.05 V, R = 0.7

The first of two tests carried out under these conditions followed a similar stepwise load reduction sequence at 5 Hz to the tests at -0.85 V. However, during one of the standard load reduction sequences, crack growth effectively stopped despite a growth rate of the order 1×10^{-8} m cycle $^{-1}$ at the previous load step. Such a sharp change in crack growth rate was not seen at the higher potential. It was found necessary to apply several stepwise increases in ΔK to restart crack growth, which then occurred suddenly at a very rapid rate and resulted in the loss of the specimen.

The test was thus repeated using smaller load reduction steps. A threshold value of 8 MPa \sqrt{m} was established at 5 Hz and the standard increasing load procedure was then applied; the results are shown in Fig. 4. However, a test interruption due to testing machine malfunction arrested crack growth at 0.167 Hz. It was not possible to resharpen the crack as similar behaviour to that of the first specimen occurred, ie crack arrest, followed eventually by a sudden and rapid increase in crack growth rate.

(d) - 1.05 V, R = 0

Results from this test are shown in Fig. 5 and include one data point from low frequency cycling. In this case leakage of seawater left the specimen dry overnight. Attempts to grow the crack and produce a fresh fracture surface at the crack tip were affected by the same problems of crack arrest and sudden acceleration as was found in the high R tests at this protection potential.

3.2 SEMI-ELLIPTICAL CRACKED SPECIMENS

Two specimens using this crack geometry have been tested, both with a protection potential of -0.85 V (SCE), one at R=0 and one at R=0.7. Crack growth in this geometry occurs along a front which requires measurement at the surface and at the deepest point to allow characterisation of the growth rate and stress intensity factor. Measurement of crack depth was made using an AC potential drop monitor. During the experimental work an assessment of the resolution of this technique was made, which suggested it was relatively insensitive compared to that required to measure low crack growth rates in a realistic time. Poor stability compared to the optical technique also caused some difficulties in controlling the load reductions applied to these specimens. These problems prevented low frequency cycling being applied to the R=0 specimen as failure occurred before a threshold growth rate could be determined under reducing ΔK at high frequency. Measurement of the surface crack length was not possible for either of these specimens due to difficulties of access and deposit obscuring the surface. The length of the surface crack was therefore found by assuming a linear relationship between the depth crack length and surface crack length determined by reference to beach marks produced on the specimen surface at intervals during the R=0.7 test. It was assumed that the R=0 test would behave in a similar manner. For the largest crack, the relationship between surface and depth crack dimensions was similar to that found by other workers (Fig. 6) confirming the basis of this approach.

The semi-elliptical cracked bend specimen with a stress ratio of 0.7 reached an apparent threshold at high frequency (5 Hz), at which point the frequency was set to 0.167 Hz. However, insufficient exposure was achieved at low frequency to produce near threshold crack growth. The low frequency growth rate values are therefore reported as upper bounds from a calculation of the number of fatigue cycles achieved and resolution of the crack monitoring technique when no crack advance had been seen to occur prior to some disruption of testing.

The semi-elliptical cracked specimen results are summarised in Table 3.

3.3 ANALYSIS OF THE SURFACE DEPOSITS IN CTS TESTS USING EPMA

The fracture surface of each of the five CT specimens was examined using a scanning electron microscope which had an energy dispersive X-ray analysis facility (Electron Probe Micro-Analysis, EPMA). This instrument enables an approximate analysis of elements with an atomic weight greater than 23 awu to be made. Each fracture surface was first examined to determine characteristic features, and then a surface analysis was made for each distinctive area. Usually these areas were in the notch, pre-crack and the fracture surface produced during the test. Results for each specimen are detailed below.

(a) Protection Potential - 0.85 V (SCE), R = 0.7

The surface film consisted of calcium with slight traces of magnesium. The deposit composition was fairly uniform over the fracture surface.

(b) Protection Potential - 0.85 V (SCE), R = 0

Particular attention was directed to the line of the beach mark which corresponded to the area of threshold testing. Like the specimen at higher R ratio, the deposit consisted mainly of calcium salts with very little magnesium being measured. Areas of about 20 μm^2 were sampled along the beach mark. The measured calcium to iron ratio was about 5:1 at either edge of the specimen but almost no iron was registered at a point within the centre of the retarded crack. The Ca:Fe ratio is an indication of deposit thickness, since the microprobe samples both the deposit and part of the substrate. A 1:1 ratio of calcium to iron was measured at the centre of the beach mark where the crack had been growing. Additional to the compositional differences between the two parts of the crack front there were differences in morphology, with needles formed at the unretarded crack line and smaller needle clusters forming spheres at the retarded line.

(c) Protection Potential - 1.05 V (SCE), R = 0.7

The surface film on this specimen showed differences in composition along the fracture. Within the notch and pre-crack areas the film consisted mainly of calcium salts, although the proportion of iron was less in the notch than the pre-crack. In contrast, the main fracture surface showed the additional presence of magnesium at an overall Mg:Ca ratio of 1:3. The morphology of this deposit consisted of a surface film containing a high proportion of magnesium overlaid by spherical nodules composed mainly of calcium.

(d) Protection Potential of - 1.05 V (SCE), R = 0

Again the notch and pre-crack surface film analysis suggested calcium salts predominated. The main fracture surface had a similar overall analysis to that tested at R = 0.7 but the film morphology was different in that it contained large and small nodules. The large nodules (about 40 μm dia.) consisted of calcium; whereas the surface and small nodules (about 5 μm dia.) consisted of about equal amounts of calcium and magnesium.

No attempt has been made to assess the full significance of these observations. However comparison of these results with those reported by Turnbull⁶ and Maahn⁷ suggests similar trends, with calcium predominating at less negative potentials (-0.85 V (SCE)) and with increased quantities of magnesium being deposited at lower potentials (-1.05 V (SCE)). Deposition of magnesium compounds in the calcareous scale formed at lower potentials is likely to be a reflection of the higher pH reached in the crack solution.

The most important overall conclusion is the presence of considerably thicker deposits for the overprotected specimens. The influence of the deposit would appear to be through a crack closure mechanism. Therefore the thickness and mechanical strength of the deposits will be expected to have the greatest influence on crack growth rates, particularly where closure becomes of increasing importance at near threshold growth rates.

4. DISCUSSION

The measurement of fatigue crack growth thresholds and near threshold growth rates provides design data under conditions during which much of the life of a structure is spent. However, generation of data in this very low crack growth rate region is extremely difficult due to the long testing times required and possible load interaction effects. Additional complication arises when measuring thresholds in a seawater environment where environmental effects may provide additional mechanisms by which the crack tip may be blunted and growth arrested.

4.1 EFFECT OF TEST PROCEDURE

Although the original function of this work was to complement and provide additional data to the work done previously, it has in practice provided an important illustration of how the measured crack growth threshold ΔK values can be influenced by the test technique. Because the method previously used to determine threshold values (stepwise decreasing load tests) has been criticised as possibly unrepresentative of behaviour in service, the work described here was performed so that near threshold growth was measured under an increasing load regime. The philosophy of this approach was that in terms of structural assessment it may be more relevant to have information concerning when a crack has begun to grow than when it has become arrested. Since it is generally accepted that a higher value of ΔK is required to start a crack growing than that at which propagation of a sharp crack is maintained, measurements made under decreasing load are often taken as a lower bound. However, the data obtained in this project indicate that this conclusion, based on tests in air, is not always applicable to corrosion fatigue in seawater, although the data are complicated by the effects of R ratio and cathodic protection potential.

4.2 EFFECT OF R-RATIO

The variation of the crack growth threshold stress intensity range (ΔK_{th}) with R-ratio is well defined for testing in air, with a scatter band for a range of mild and low alloy steels as shown in Fig. 7 from data compiled by Lindley and Richards⁸. This compilation of data for BS4360:50D steel from a number of workers^{2,9,10} includes a data set² for the cast tested here. The shape of the bounding curves suggests that there is a relationship between increasing R-ratio and decreasing values of ΔK_{th} . However, work done by Radon¹⁰ suggests that this trend may be due to thickness effects since the higher values of ΔK_{th} at low R were reduced to values closer to those at high R when thicker specimens were tested. However, work by Bathias¹¹ on an aluminium alloy does not support this conclusion, although the range of specimen thicknesses in this work did not include the thickest geometry studied by Radon.

The effect of introducing a corrosive environment serves to add further mechanisms controlling crack propagation and arrest to the fatigue process which occurs in air. Figure 8 shows data from a number of workers obtained under decreasing ΔK conditions in seawater with and without cathodic protection, plotted on the scatter band obtained for BS4360 50D air data. One result from the previous UK work, under decreasing load at R = 0.5 indicates a reversed trend to that of the air data where, in seawater under cathodic protection at - 0.85 V (SCE) ΔK_{th} increases with increasing R-ratio. Contrasting with this result are the increasing ΔK data obtained in this study which exhibit a similar trend to the air data (i.e. lower ΔK_{th} with increasing R-ratio). The R = 0.7 threshold measured under optimum cathodic protection (-0.85 V) in the current programme is only slightly above that in air, in contrast to the much increased ΔK_{th}

values (at $R=0.5$) measured under decreasing ΔK conditions. This ΔK_{th} is much below the value which might have been predicted from extrapolation of the decreasing ΔK data at $R=0$ and 0.5 . Further evidence for the importance of test procedure is provided by the wide scatter in reported data at $R=0.5$ (Fig. 8).

At low R , close to $R=0$, the effect of seawater under optimum cathodic protection or freely corroding conditions is negligible compared to air data under both increasing or decreasing ΔK testing. This latter observation may be due to the important contribution of crack closure in determining the value of ΔK_{th} at low R ratio. Where closure occurs, induced either from plasticity or roughness effects, scale formation is likely to be inhibited due to mechanical cleaning of the mating surfaces. Hence at low R , where mechanical closure has a large influence and scale formation is effectively prevented, threshold values are close to those in air. Where mechanical closure has a reduced influence, scale formation can occur and increase closure. Under decreasing load conditions scale formed at high load becomes more effective in blocking the crack as the load is reduced, increasing the value of measured threshold.

4.3 EFFECT OF CATHODIC PROTECTION POTENTIAL

Substantially different behaviour is observed under cathodic overprotection conditions, where heavy scale formation dominates low ΔK crack growth behaviour as shown by the EPMA measurements. This resulted in crack arrest occurring unpredictably even during testing at 5 Hz, at both $R=0$ and $R=0.7$, even at high values of ΔK ($14 \text{ MPa}\sqrt{\text{m}}$ at $R=0$, $8 \text{ MPa}\sqrt{\text{m}}$ at $R=0.7$) (Fig. 8). Following crack arrest a substantial increase in ΔK was necessary to restart crack growth, but when this occurred it proceeded at a rapid rate.

Crack arrest is presumably due to a reduction in the effective stress intensity range, even at high R ratio. The exact stress intensity level at which crack growth stops may depend as much on prior test history and exposure time as on the value of threshold measured under scale-free conditions. Measurement of the effective stress intensity range e.g. by measuring crack opening displacement, may provide a rational basis for ΔK_{th} determination under these conditions. There is also an uncertainty as to how effective calcareous deposits would remain under compressive loading in reducing the effective ΔK value, and hence crack growth rates. Unless it is possible to guarantee that disruption of such deposits cannot occur, it may be more realistic to use threshold crack growth data from scale free conditions. Such data could be obtained, for example, from tests in sodium chloride solution.

4.4 EFFECT OF SPECIMEN GEOMETRY

The data obtained during this test programme included a limited number of results using specimens containing semi-elliptical cracks tested under bending. Many of the data were obtained at high frequency (5 Hz) although an estimate of near threshold growth rate was obtained from low frequency testing (0.167 Hz). The results obtained from the high R specimens suggest considerable differences between the crack growth rates at the higher frequency under reducing load compared to the estimated growth rates at low frequency under increasing load. Although these data are broadly similar to those from compact tension specimens, they are not sufficiently complete to be able to confirm the lack of an effect of specimen geometry. No published data on specimens of similar geometry have been located. Threshold measurements have, however, been reported on through-thickness notched bend specimens, e.g. Bardal⁹ used multiple edge notched specimens, again at relatively high

frequency (1 Hz). His results shown in Figure 8 indicate somewhat lower threshold values at R of 0.05 and 0.5 than results from CTS geometry, although they are within the scatter band of air data. The work of Booth¹³ using SEN specimen geometry at 0.167 Hz resulted in a ΔK_{th} at R = 0.05 which was in close agreement with Bardal's data, although no high R results were produced. Insufficient data are available to provide a detailed comparison between different specimen geometries over a range of R ratio, although comparison between CTS and SEN data suggests some dependence on specimen type may occur. Further work using more realistic crack shapes e.g. semi-elliptical cracks would be of considerable value in assessing the importance of crack geometry on threshold measurements in seawater environments.

Recent progress in the understanding of fatigue crack growth thresholds has led to standard test methods being formulated to measure thresholds in a consistent and reliable way¹⁴. The aim of many of these methods is to allow repeatable measurements to be made in air or an inert environment. However the results of the preliminary work reported here suggest that these techniques may be less relevant to testing in seawater, particularly under cathodic protection where scale formation can occur and reduce the effective ΔK . Additionally, these standards apply to a limited number of specimen geometries including CTS and SEN, which raises the question as to which is the most relevant to practical conditions. Further work using semi-elliptical cracked specimens may be beneficial in providing data from cracks which do not have open sides. Recent work on the electrochemistry in corrosion fatigue cracks in seawater suggests the mechanism for enhanced crack growth at potentials more positive than about -1.0 V (SCE) may be due to hydrogen generated at the crack tip⁶. Where the crack front intersects the specimen surface, hydrogen generated at that surface could more readily diffuse to the edges of a through crack, enhancing growth rates compared to those in semi-elliptically cracked specimens.

5. CONCLUSIONS

The following conclusions may be drawn from the present work, although, due to the exploratory nature of this increasing ΔK test programme, these must be considered tentative.

1. Corrosion fatigue testing of compact tension specimens of BS4360:50D steel in natural seawater indicated that the measured corrosion fatigue threshold ΔK (ΔK_{th}) was influenced by several interacting variables, such as protection potential, applied load ratio, and test procedure (i.e. increasing vs decreasing ΔK).
2. Under optimum cathodic protection (-0.85 V SCE) and low stress ratios where crack closure is important, there was only a small increase of ΔK_{th} compared to that measured in air. Thresholds measured under increasing or decreasing ΔK conditions were quite similar. However, at high stress ratios there was a marked effect of the method of testing with a much higher ΔK_{th} being predicted for decreasing ΔK conditions. Thresholds measured in air, or under increasing ΔK conditions in seawater, showed a reduction with increasing stress ratio (by about a factor of 2 between $R=0$ and 0.7). Overall, thresholds in seawater were about 20% higher than in air. However, thresholds measured under decreasing ΔK conditions in seawater were very much higher at high R .
3. Under cathodic overprotection (-1.05 V SCE), the formation of calcareous deposits dominated crack growth at low values of ΔK . Thus, measured threshold values could be considerably higher than at more positive protection potentials. The exact value is likely to be very dependent on the specimen test history, but its determination is difficult since formation of scale may lead to premature crack arrest. Even at less negative potentials, unpredictable calcareous deposits may lead to variable or localised crack arrest. The proportion of magnesium in the scale is greater at the more negative potentials.
4. Near threshold crack growth rates from semi-elliptical cracked bend specimens fatigue cycled at 5 Hz suggest rates of the same order as rates from through thickness cracked (compact tension) specimens. However, this test frequency is higher than that at which a significant influence of environment is expected. Therefore, this conclusion is not necessarily applicable to the low frequencies which are more important under practical conditions and where crack shape may have greater significance.

6. RECOMMENDATIONS

1. The results reported here suggest that the very high thresholds found under reducing ΔK conditions² may be inapplicable under the increasing ΔK conditions likely to be more relevant to real structures. This conclusion is based on just two tests at -0.85V SCE, and so requires confirmation over a range of R ratios and at free corrosion and overprotection potentials.
2. Crack growth thresholds appear to be higher under cathodic over-protection conditions ($\approx 1.05V$ SCE) than at more positive potentials, due to calcareous scale formation. Tests at negative R ratios are required to ensure this calcareous scale would remain intact under compressive loading.
3. Due to the large observed influence of calcareous scale on crack growth, and particularly on the arrest of growing cracks, more detailed microstructural examination is recommended on the specimens tested in this programme.
4. Because calcareous scale formation dominates observed crack growth behaviour under cathodic protection, it is not possible to state with certainty what crack growth rates might be if this scale were not present. In work done previously using sodium chloride environments, eg Vosikovsky¹⁵ to measure fatigue thresholds in steel exposure times were relatively short, hence the full influence of hydrogen on crack growth rates may not have been seen. Long term tests in sodium chloride are therefore recommended to ensure that hitherto unmeasured high crack growth rates could not occur in practice if the scale was disrupted.
5. Recent experimental work on the electrochemistry in corrosion fatigue cracks in seawater suggests a hydrogen based mechanism of cracking may be dominant, and that hydrogen levels may build up in components over relatively long periods (approx. 1 year)¹⁶. Some corrosion fatigue tests are therefore recommended on specimens which have been previously immersed in seawater under cathodic protection for relevant periods.
6. The two exploratory tests on semi-elliptical cracked specimens were inadequate to generate reliable crack growth data in the threshold region. Further testing is recommended to assess the effect of crack geometries more relevant to real structures, using a more sensitive and stable method of crack monitoring.

7. REFERENCES

1. D TAYLOR. A compendium of Fatigue Thresholds and growth rates, EMAS 1985.
2. H G MORGAN. The determination of fatigue thresholds and short crack behaviour in structural steel to BS4360:50D in air and seawater. ND-R-985(S) 1985.
3. British Standards Institution. Welding Structural Steel, BS4360 1972.
4. P M SCOTT and T W THORPE. Prediction of Semi-elliptic Crack Shape Development during Fatigue Crack growth. AERE-R-10104 1981.
5. WD DOVER, F D W CHARLESWORTH, K A TAYLOR, R COLLINS and D H MICHAEL. A C Field Measurement: Theory and Practice. In "The measurement of Crack Length and Shape during fracture and Fatigue". Ed C J Beevers. EMAS 1986.
6. A TURNBULL and D H FERRIS. Mathematical Modelling of the Electrochemistry in Corrosion Fatigue Cracks in Structural Steel Cathodically protected in Seawater. Corrosion Science, 26 8 p601-628 1986.
7. E MAAHN. Environmental Effects in Fatigue Crack Initiation and Propagation. Technical Report No. 5, project 7210. KG/902 1st July - 31st December 1986.
8. T C LINDLEY and C E RICHARDS. Near threshold fatigue crack growth in materials used in the electricity supply industry. Proceeding of an Int. Conf. on Fatigue Thresholds - Stockholm June 1981 Ed C J Beevers et al, EMAS 1982.
9. E BARDAL et al. Measurements of Very low Corrosion Fatigue Crack growth rates in Structural Steel in Artificial Seawater Ref. 7.
10. J RADON. Fatigue Crack Growth in the Threshold Region Ref. 7.
11. C BATHIAS, A PINEAU, J PLUVINAGE and P RABBE. Fracture 1977 Vol. 2 ICF4 Waterloo, Canada June 19-24 1977 p1283-1286.
12. I M AUSTEN. Steel in Marine Structures Conference, Delft, June 1987.
13. G S BOOTH, J G WYLDE and I IWASAH. Fatigue 1984, Proc. Int. Conf., Birmingham, Sept 1984 3 p1471-1484.
14. Draft DD on the measurement of threshold stress intensity values and fatigue crack growth rates in metallic materials. BSI 86/44783 (1986).
15. O VOSIKOVSKY. Frequency, Stress Ratio and Potential Effects on Fatigue Crack Growth of HY 130 Steel in Salt Water. J Testing and Eval. 1978, 6 pp175-182.
16. A TURNBULL and M SAENZ de SANTA MARIA. Modelling of crack-tip deformation and transient electrochemical processes in relation to corrosion fatigue of steels cathodically protected in marine environments. NPL Report DMA(A)145, April 1987.

TABLE 1**CHEMICAL COMPOSITION AND MECHANICAL PROPERTIES OF BS4360 50D STEEL**

Chemical Analysis	Weight Percent
Carbon	0.18
Silicon	0.36
Manganese	1.35
Niobium	0.03
Vanadium	0.01
Sulphur	0.024
Phosphorus	0.038

Mechanical Properties	
Yield Strength	370 MPa
UTS	540 MPa
Elongation	31%
Charpy Energy at - 30°C	116 J

TABLE 2

THE COMBINATION OF STRESS RATIO AND PROTECTION POTENTIAL CONDITIONS INVESTIGATED IN REF 2 AND THIS STUDY USING NATURAL SEAWATER AT 7°C

Protection Potential:	Free Corrosion	-0.85 V (SCE)	-1.05 V (SCE)
Stress Ratio			
0	*	*0+	0
0.5	*	*	
0.7		0	0

* = Tests performed in previous work²

0 = Tests performed in this study

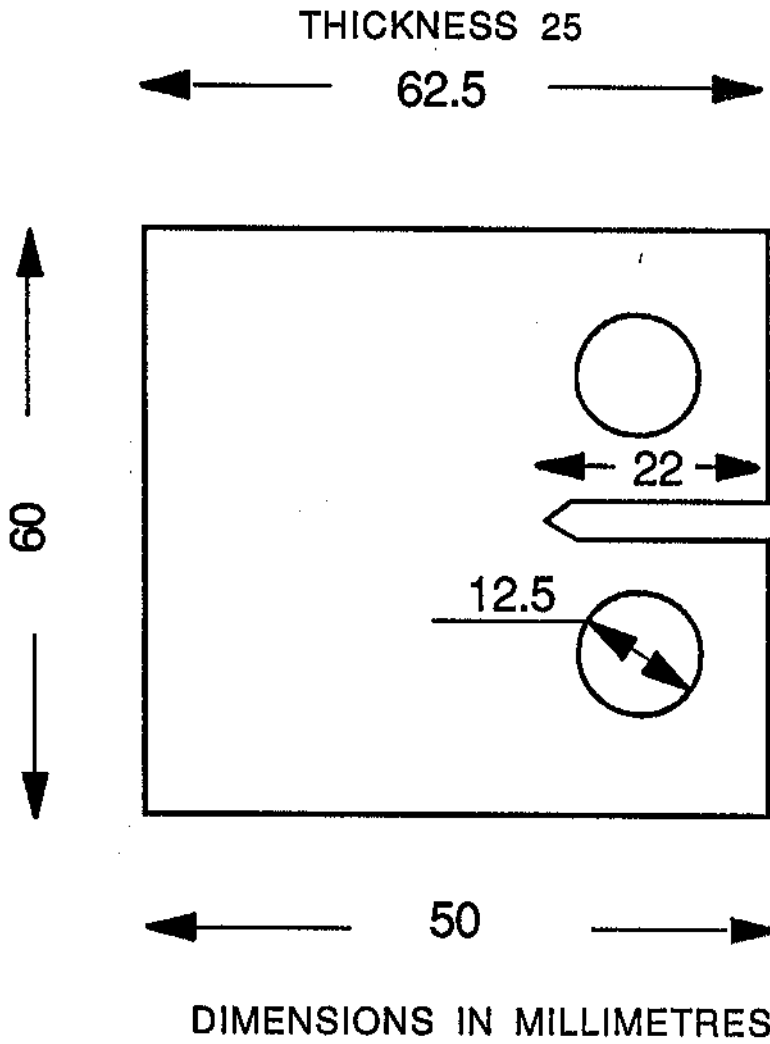
+ = This test was originally due to be run with a stress ratio of - 1.0 but was changed in light of early results to provide a direct comparison with previous work

TABLE 3

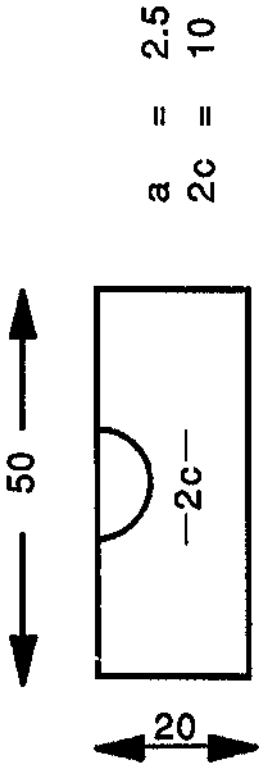
CRACK GROWTH RATES IN THE DEPTH DIRECTION
FROM SEMI-ELLIPTICAL CRACK SPECIMENS
EXPOSED TO SEAWATER WITH CATHODIC
PROTECTION AT - 0.85 V (SCE)

Surface ΔK MPa \sqrt{m}	Depth ΔK MPa \sqrt{m}	Cyclic Crack Growth Rate m Cycle ⁻¹
<u>R=0.7</u>		
<u>5 Hz Reducing Load</u>		
8.62	7.5	1.5×10^{-10}
8.54	7.52	5.5×10^{-10}
<u>0.167 Hz Increasing Load</u>		
6.18	5.15	$< 7.5 \times 10^{-10}$
6.78	5.62	$< 4.7 \times 10^{-9}$
<u>R=0</u>		
<u>5 Hz Reducing Load</u>		
11.0	9.0	2.7×10^{-10}
11.4	9.3	3.2×10^{-10}

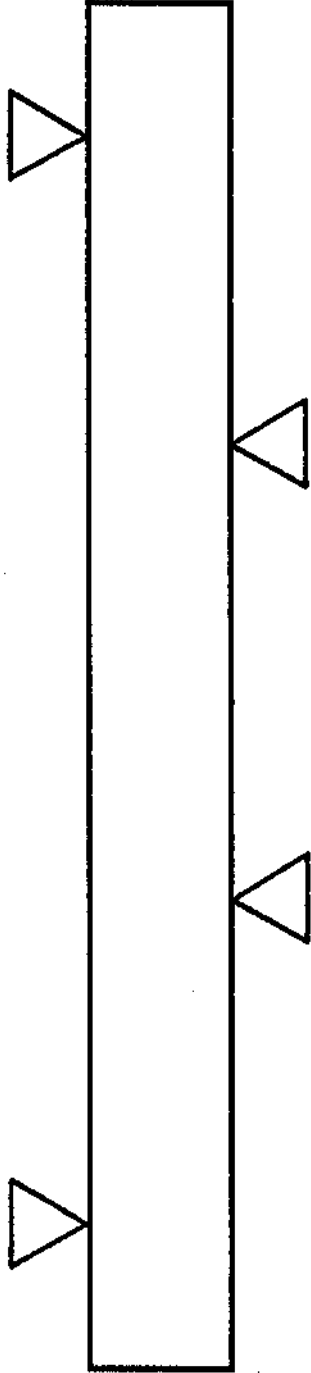
FIG 1 COMPACT TENSION SPECIMEN



SECTION THROUGH SPECIMEN



OUTER LOAD POINT 200



DIMENSIONS IN MILLIMETRES INNER LOAD POINT 80

FIG 2 SEMI-ELLIPTICAL CRACKED SPECIMEN

FIG 3 NEAR THRESHOLD CRACK GROWTH RATES IN BS 4360 STEEL IN SEA WATER UNDER CATHODIC PROTECTION AT -0.85 v (SCE)

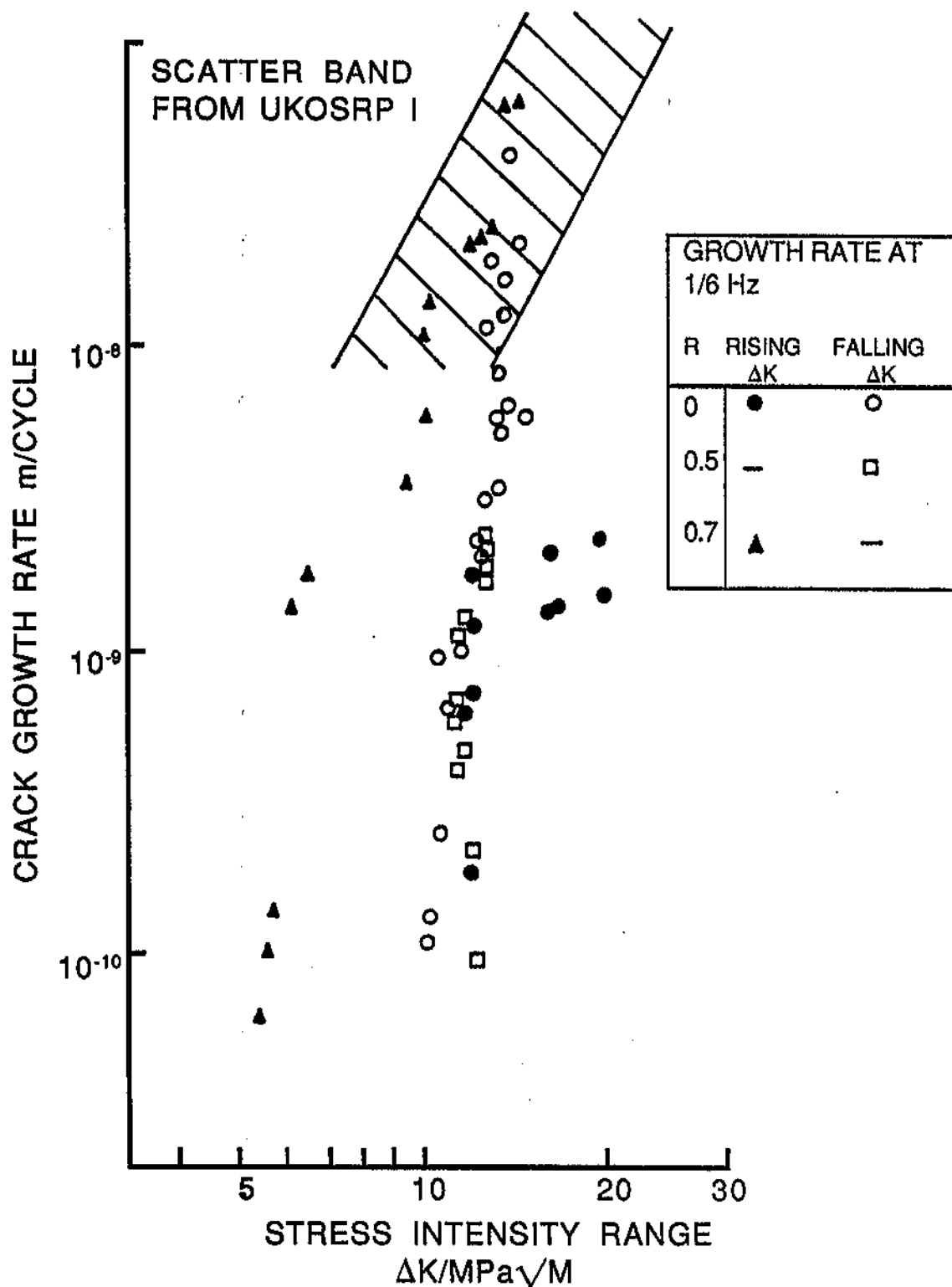


FIG 4 NEAR THRESHOLD CRACK GROWTH RATES IN BS 4360 50D STEEL IN SEA WATER UNDER CATHODIC PROTECTION AT - 1.05 V(SCE) AND STRESS RATIO 0.7

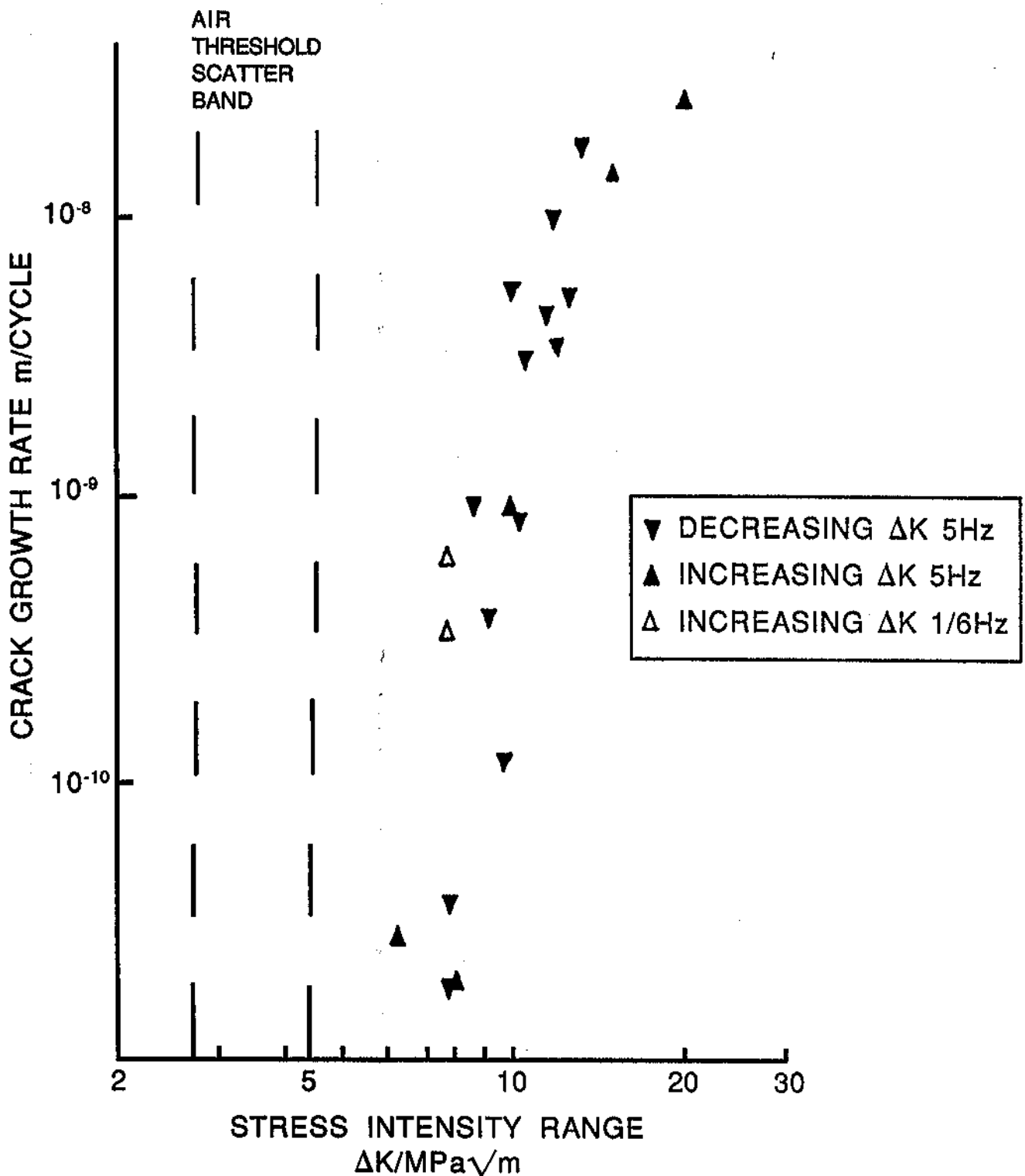


FIG 5 NEAR THRESHOLD CRACK GROWTH RATES IN BS 4360 50D STEEL IN SEA WATER UNDER CATHODIC PROTECTION AT - 1.05 V (SCE) AND STRESS RATIO 0

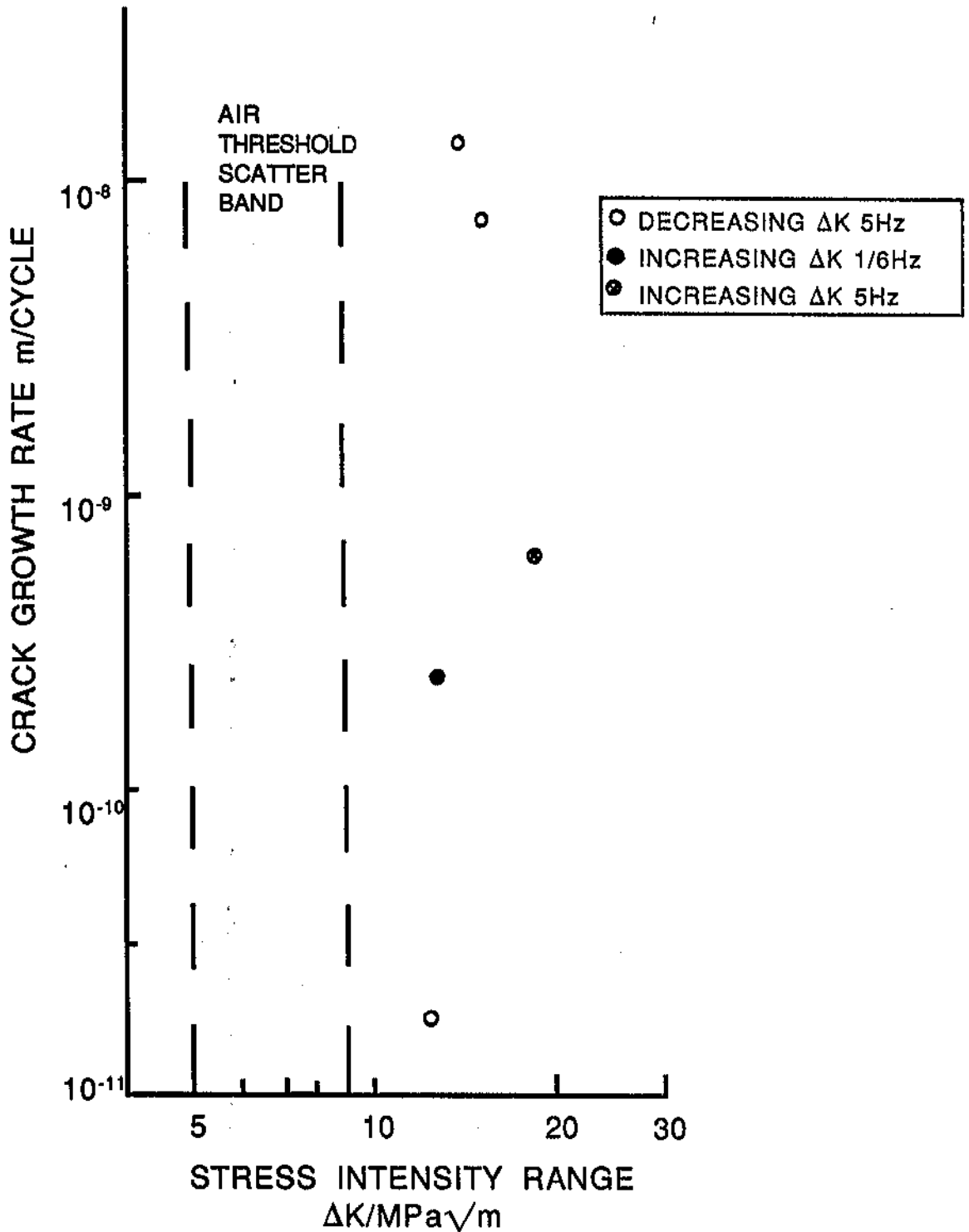


FIG 6 DEVELOPMENT OF CRACK SHAPE UNDER BENDING, FATIGUE LOADING

- DATA FROM THORPE et al - 'FATIGUE IN OFFSHORE STRUCTURAL STEELS' INST OF CIVIL ENGINEERS 24-25 FEB 1981
- DATA FROM PORTCH CEGB REPORT RB/B/N4645
- ▲ DATA FROM THIS WORK

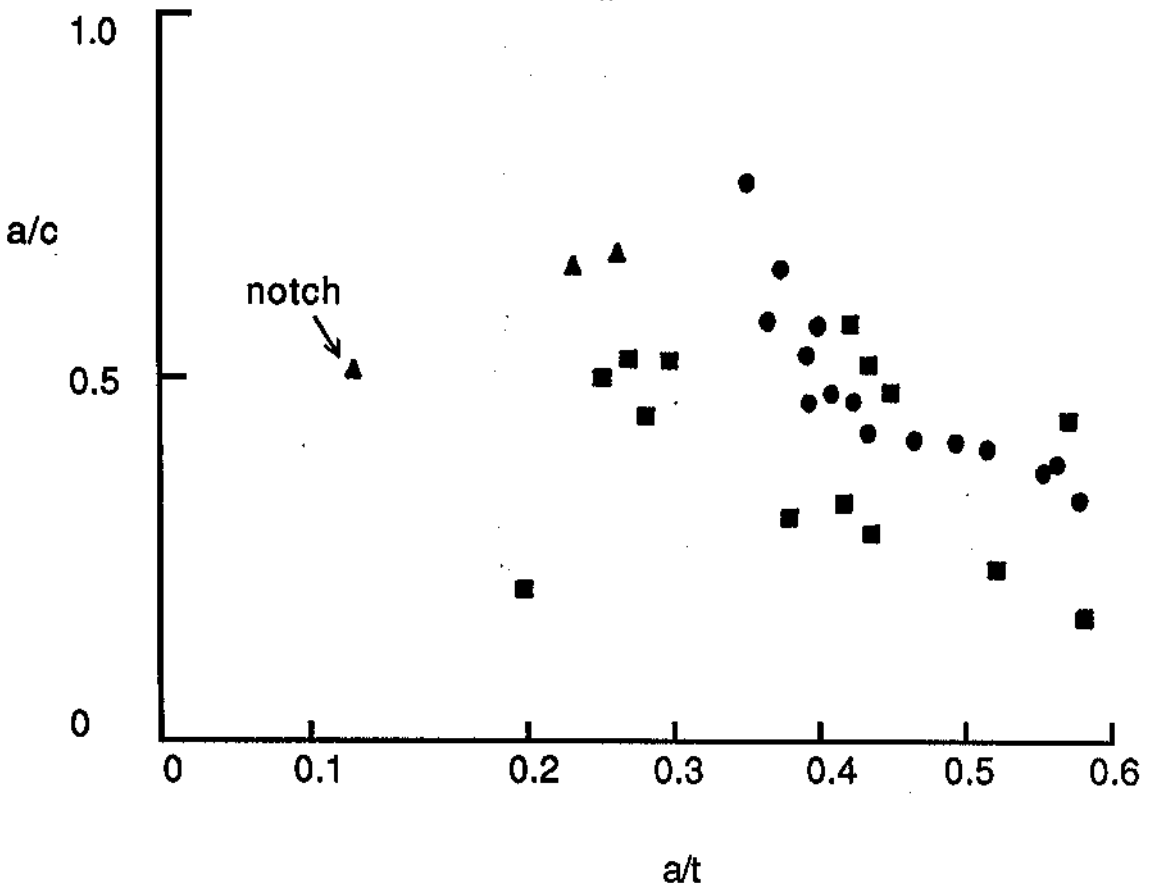
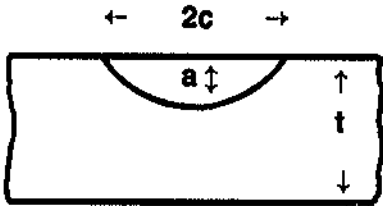


FIG 7 VARIATION OF THRESHOLD STRESS INTENSITY RANGE WITH STRESS RATIO IN STRUCTURAL STEELS IN AIR, DISCRETE POINTS FOR BS 4360 50D STEEL

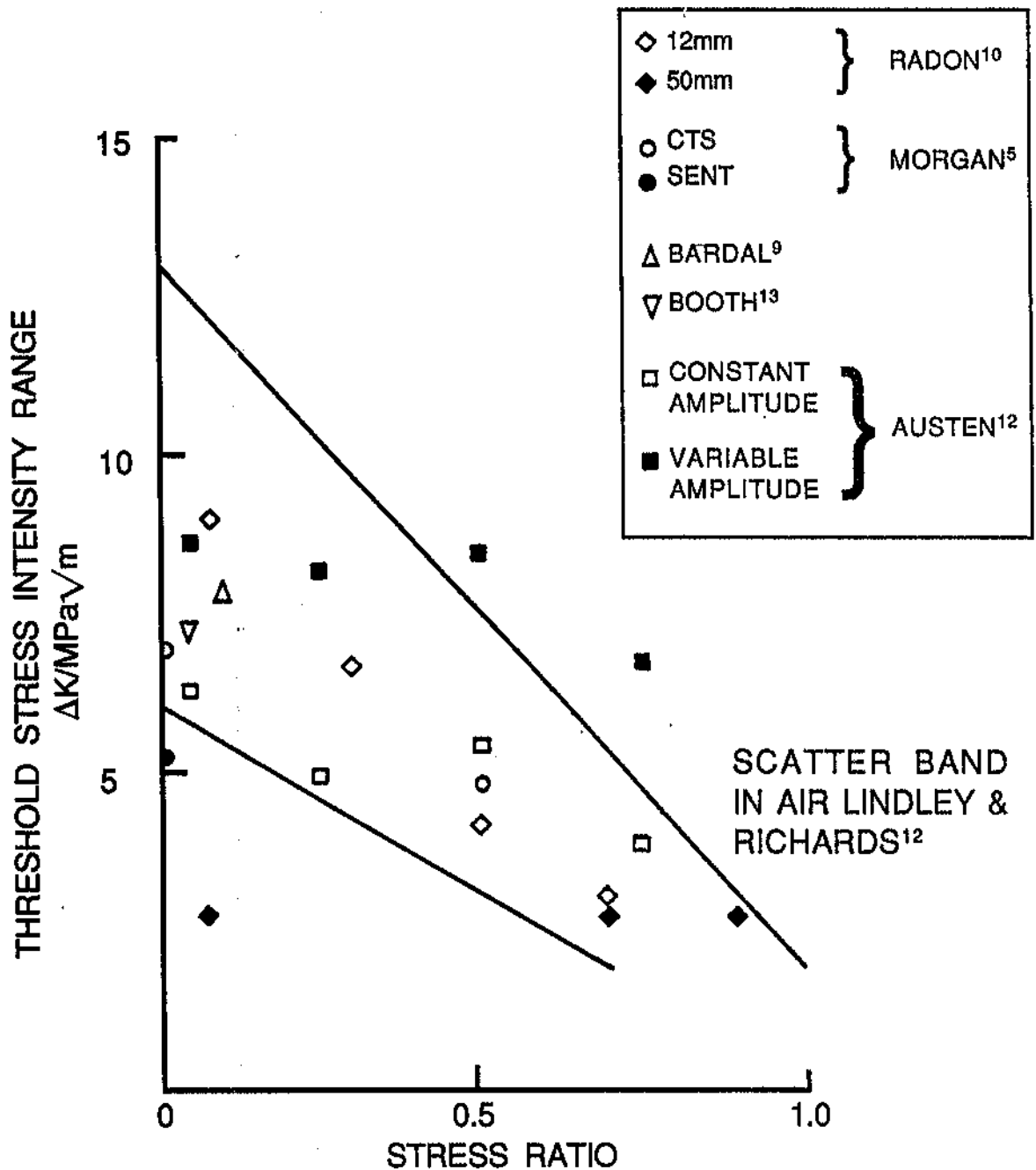
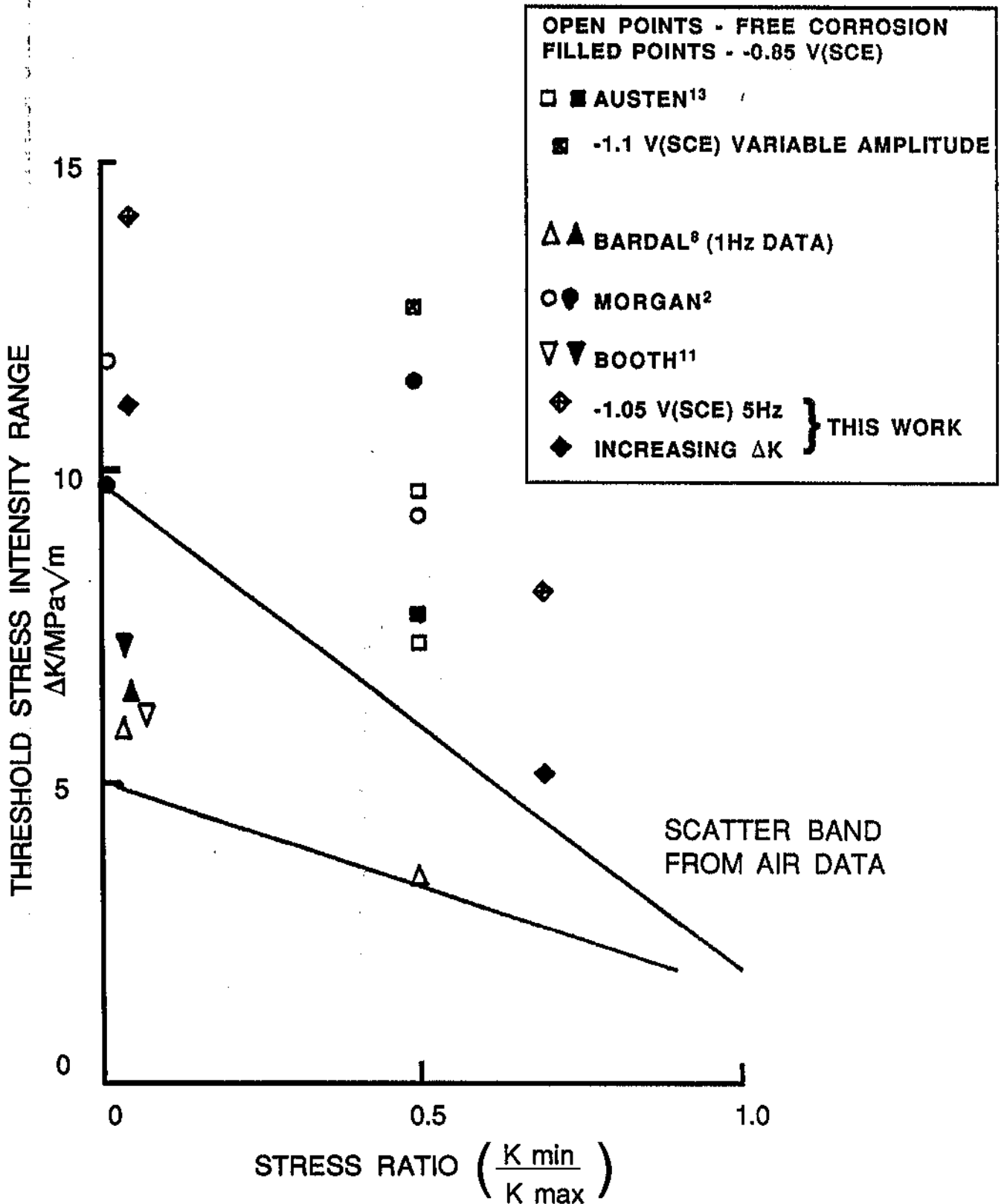


FIG 8 VARIATION OF THRESHOLD STRESS INTENSITY RANGE WITH STRESS RATIO IN BS 4360 50D STEEL IN SEA WATER





HMSO publications are available from:

HMSO Publications Centre

(Mail and telephone orders only)

PO Box 276, London, SW8 5DT

Telephone orders 071-873 9090

General enquiries 071-873 0011

(queuing system in operation for both numbers)

HMSO Bookshops

49 High Holborn, London, WC1V 6HB 071-873 0011 (counter service only)

258 Broad Street, Birmingham, B1 2HE 021-643 3740

Southey House, 33 Wine Street, Bristol, BS1 2BQ (0272) 264306

9-21 Princess Street, Manchester, M60 8AS 061-834 7201

16 Arthur Street, Belfast, BT1 4JY (0232) 238451

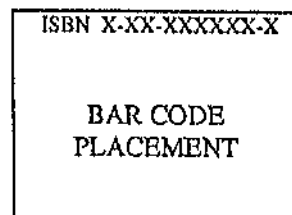
71 Lothian Road, Edinburgh, BH3 9AZ 031-228 4181

HMSO's Accredited Agents

(see Yellow Pages)

and through good booksellers

£xx.xx net





HMSO publications are available from:

HMSO Publications Centre

(Mail and telephone orders only)

PO Box 276, London, SW8 5DT

Telephone orders 071-873 9090

General enquiries 071-873 0011

(queuing system in operation for both numbers)

HMSO Bookshops

49 High Holborn, London, WC1V 6HB 071-873 0011 (counter service only)

258 Broad Street, Birmingham, B1 2HE 021-643 3740

Southey House, 33 Wine Street, Bristol, BS1 2BQ (0272) 264306

9-21 Princess Street, Manchester, M60 8AS 061-834 7201

16 Arthur Street, Belfast, BT1 4JY (0232) 238451

71 Lothian Road, Edinburgh, EH3 9AZ 031-228 4181

HMSO's Accredited Agents

(see Yellow Pages)

and through good booksellers

£xx.xx net

